risks

MDPI

Article

Corporate Debt as a Put Option: A Structural Credit Risk Framework for Banks Under Dynamic Refinancing Risk

Vukosi Era Maluleke [1,*], Eben Maré [2] and Conrad Beyers [1]

[1] Department of Actuarial Science, University of Pretoria, Pretoria 0002, South Africa; conrad.beyers@up.ac.za
[2] Department of Mathematics and Applied Mathematics, University of Pretoria, Pretoria 0002, South Africa; eben.mare@up.ac.za
* Correspondence: vukosiera@hotmail.com; Tel.: +27-82-358-9818

Abstract

This paper extends the classical Merton structural credit risk model by incorporating dynamic refinancing risk into the measurement of bank default risk. The study addresses a key limitation of traditional structural models, which treat default as a function of asset values relative to liabilities but abstract from debt maturity structure and rollover conditions. The proposed framework integrates an issuance-based refinancing ladder, a market-consistent funding curve, and firm-level balance sheet data within a liquidity-adjusted structural model featuring an endogenous default barrier and a refinancing-adjusted distance-to-default measure. Using bank-level data (1564 daily observations, 2020–2026), the results show that, although the institution remains solvent under conventional structural measures, refinancing exposure materially compresses the effective solvency buffer. Short-term refinancing exposure averages R8.1 billion and reaches approximately R19.6 billion during stress periods; the liquidity-adjusted distance to default averages 1.47 (range 0.46–2.15) and the implied probability of default averages 9.5% (range 1.6–32.2%). A Newey–West heteroskedasticity- and autocorrelation-consistent regression that controls for asset volatility and the underlying solvency ratio confirms that the refinancing ratio has a negative and highly statistically significant partial effect on distance to default (coefficient -1.95, t = -7.41, $p < 0.001$, N = 1564), isolating the liquidity-adjustment channel from concurrent changes in volatility and balance sheet solvency. Stress testing further reveals nonlinear amplification of default risk when funding and refinancing shocks interact. The findings indicate that bank default risk is driven not only by leverage, but also by the interaction between asset values, liability structure, and funding conditions, with implications for credit risk modelling, stress testing, and prudential risk management.

Keywords: structural credit risk; Merton model; refinancing risk; bank funding; liquidity risk; distance to default; default probability

Check for updates

Academic Editors: Tak Kuen Ken Siu and Hailiang Yang

Received: 18 July 2026
Revised: 10 August 2026
Accepted: 18 August 2026
Published: 23 August 2026

1. Introduction

The measurement of default risk remains one of the central problems in financial risk management. For both financial institutions and regulators, the ability to assess the likelihood of distress is fundamental to pricing credit risk, allocating capital, conducting stress testing, and maintaining financial stability. Structural credit risk models provide one of the most influential theoretical frameworks for addressing this problem by linking firm value, capital structure, and default risk within an option-theoretic setting. The seminal model of Merton (1974) interprets equity as a call option on firm assets, with default occurring when asset values fall below the face value of debt at maturity. This framework has profoundly shaped modern credit risk theory and motivated a large literature extending its assumptions and applications. Subsequent developments expanded the structural approach through endogenous default triggers, optimal capital structure, and empirical implementations such as the KMV framework (Black and Cox 1976; Leland 1994; Leland and Toft 1996; Crosbie and Bohn 2003; Bharath and Shumway 2008; Vassalou and Xing 2004).

Regulatory practice already recognises liquidity as a dimension of bank soundness that is distinct from solvency and is not fully captured by balance sheet leverage alone. Prudential supervisors commonly assess bank health using a CAMELS-type framework—capital adequacy, asset quality, management quality, earnings, liquidity, and sensitivity to market risk—in which liquidity (the "L") is scored separately from capital adequacy (the "C"), precisely because a bank can appear solvent on a balance sheet basis while remaining acutely exposed to funding and rollover pressure (Gilbert et al. 2000). The failure of African Bank Limited in 2014 illustrates this distinction concretely: applying a Merton-type structural distance-to-default measure to African Bank's market data, Sanderson et al. (2017) show that funding and liquidity pressure were material to the bank's deterioration in ways not fully anticipated by solvency-based supervision and disclosure at the time. This regulatory and empirical precedent motivates treating refinancing and liquidity risk as an explicit, separately modelled channel of default risk, rather than folding it implicitly into a single solvency-based structural measure, which is the approach developed in this paper.

Despite these advances, an important limitation remains. Most structural models treat liabilities as a homogeneous claim or assume a simplified debt structure, abstracting from the maturity profile of debt and the dynamics of funding rollover. This is particularly restrictive in banking, where maturity transformation creates an inherent exposure to liquidity and refinancing risk (Diamond and Dybvig 1983). While traditional structural models focus on solvency risk, theory and crisis evidence show that distress may emerge through funding disruptions even before balance sheet insolvency. Gorton (2010), Gorton and Metrick (2012), Brunnermeier and Oehmke (2013), He and Xiong (2012), Acharya et al. (2014), Brunnermeier and Pedersen (2009), and Huang and Ratnovski (2011) all highlight that default risk is jointly determined by asset values, liability structure, and funding conditions, rather than leverage alone.

Empirical evidence from financial crises reinforces this view. Bernanke (2013), Duffie (2010), and Krishnamurthy et al. (2014) document how stress in short-term funding markets can materially weaken financial institutions. At the same time, funding conditions are inherently state-dependent, evolving with interest rates, term premia, liquidity conditions, and credit spreads. Classical term structure models (Vasicek 1977; Cox et al. 1985; Hull and White 1990), together with empirical decompositions of yields (Adrian et al. 2013), imply that funding costs should not be treated as static parameters. Related evidence also shows that liquidity and funding constraints are directly priced in credit markets (Longstaff et al. 2005; Acharya et al. 2013), while Basel III liquidity standards explicitly recognise vulnerabilities arising from excessive short-term funding dependence (BCBS 2013). More recent evidence further shows that borrowing costs, global liquidity conditions, and funding shocks materially affect risk transmission and refinancing vulnerability (Acharya and Steffen 2020; Haddad et al. 2021; Miranda-Agrippino and Rey 2020; Bauer and Rudebusch 2020; Jiang et al. 2021; Eren et al. 2020).

Despite substantial progress across structural, liquidity, and regulatory studies, relatively few models integrate dynamic refinancing risk directly into structural credit risk frameworks in a tractable and empirically implementable manner. Existing structural models prioritise analytical tractability but abstract from liability dynamics, while liquidity-

https://doi.org/10.3390/risks14090189

focused approaches often lack the balance sheet intuition of structural models. This creates a gap between theoretical credit risk modelling and practical risk management needs.

This paper addresses that gap by extending the Merton framework to incorporate dynamic refinancing risk in a banking context. Specifically, the paper introduces a liquidity-adjusted structural framework featuring an endogenous default barrier, a dynamic refinancing ladder constructed from issuance data, and a market-consistent funding curve reflecting time-varying borrowing costs. These elements are combined to construct a liquidity-adjusted distance-to-default measure that explicitly links refinancing pressure to default risk.

This study is organised around three explicit research questions. RQ1: does explicitly incorporating an issuance-based refinancing ladder and a market-consistent funding curve into a Merton-type structural model produce a materially different, and theoretically correctly signed, measure of default risk relative to the classical (non-liquidity-adjusted) structural benchmark? RQ2: does refinancing pressure have a statistically significant, independent (partial) effect on liquidity-adjusted distance to default once asset volatility and the underlying solvency ratio are held constant, or does any apparent relationship reduce to a confound of these other channels? RQ3: how do funding shocks and refinancing shocks interact under joint stress, and is the interaction linear or amplifying? These questions are answered empirically in Sections 4.2–4.8: RQ1 and RQ2 are addressed through the direct benchmark against the classical Merton measure and the Newey–West regression of Section 4.6, and RQ3 through the stress testing analysis of Section 4.5.

Regarding empirical validation, this paper distinguishes between two forms of evidence. Model-implied illustrations describe outputs that follow, by construction, from the model's functional form and calibration (for example, the fact that distance to default falls when the refinancing ratio rises is partly mechanical given Equation (13)). Independent validation would require predictive testing against external, out-of-sample outcomes such as realised defaults, rating downgrades, or credit-default-swap spreads. Because the empirical application is necessarily restricted to a single, currently solvent institution over a sample containing no default event (a direct consequence of the confidentiality constraints under which the underlying commercial data were made available), formal discrimination-based validation (ROC/AUC, Brier scores against realised defaults) is not feasible here. The paper therefore reports (i) a classical-model benchmark, (ii) a confound-controlled regression test of the refinancing channel, and (iii) an external market-consistency check against observed issuance spreads, and is transparent that these constitute model-implied illustrations and internal-consistency evidence rather than out-of-sample predictive validation; the formal validation and robustness evidence supporting this is presented in Section 4.6, and this constraint is discussed further in the Limitations (Section 5).

The central premise is that default risk in banks is driven not solely by leverage or asset volatility, but by the interaction between asset values, liability structure, and funding conditions. The contribution of this paper is threefold. First, it extends structural credit risk theory by embedding dynamic refinancing risk directly within a Merton-type framework. Second, it introduces an empirically tractable methodology for measuring refinancing pressure using issuance-based maturity profiles and market-consistent funding conditions. Third, it demonstrates empirically that incorporating liability structure materially alters measured default risk, thereby improving the relevance of structural credit models for risk management, stress testing, and prudential analysis.

https://doi.org/10.3390/risks14090189

2. Related Work

2.1. Structural Credit Risk, Liquidity, and Refinancing Risk

Structural credit risk models provide the foundation for analysing default risk by linking solvency to the relationship between asset values and liabilities. The seminal framework of (Merton 1974), together with extensions by (Black and Cox 1976), (Leland 1994), and (Leland and Toft 1996), established the theoretical basis for modelling default through endogenous or boundary-based mechanisms. Empirical implementations such as (Crosbie and Bohn 2003), as well as evidence from (Vassalou and Xing 2004) and (Bharath and Shumway 2008), show the practical relevance of structural models for measuring distance to default. However, these approaches generally abstract from the maturity structure of liabilities and the role of dynamic refinancing conditions.

The parallel banking and liquidity literature shows that this omission is particularly important for financial institutions. Banks face inherent liquidity risk due to maturity transformation (Diamond and Dybvig 1983), while funding structure and wholesale market dependence materially influence fragility (Allen and Gale 2000; Freixas and Rochet 2008; Huang and Ratnovski 2011). More recent theoretical contributions show that leverage, short-term funding, and rollover exposure can generate endogenous liquidity risk and amplify default risk (Acharya and Viswanathan 2011; Morris and Shin 2010; He and Xiong 2012; Brunnermeier and Oehmke 2013). Crisis evidence further reinforces this view, with disruptions in wholesale funding markets shown to be central to financial instability (Gorton 2010; Brunnermeier 2009; Gorton and Metrick 2012; Duffie 2010; Krishnamurthy et al. 2014).

Taken together, this literature suggests that default risk in banks cannot be understood solely through solvency-based frameworks, but must incorporate the interaction between asset values, liability structure, and refinancing conditions.

Critically, these two strands of literature differ methodologically in ways that matter for the present study. The structural tradition (Merton 1974; Black and Cox 1976; Leland 1994; Leland and Toft 1996) is analytically tractable and produces closed-form or near-closed-form default probabilities, but generally treats the default barrier as either a fixed face value of debt or an endogenously optimised trigger chosen at issuance, which is not designed to respond to short-run changes in rollover conditions. Empirical implementations such as Crosbie and Bohn (2003) and Bharath and Shumway (2008) improve empirical tractability by using equity market information directly, at the cost of abstracting further from the liability side of the balance sheet. The liquidity and banking literature (Diamond and Dybvig 1983; He and Xiong 2012; Brunnermeier and Oehmke 2013) is, by contrast, primarily theoretical and equilibrium-based, offering rich intuition for why rollover risk should matter but rarely producing a directly estimable, firm-level default risk measure that a risk manager could compute from observable data. The framework proposed in this paper is positioned explicitly at this methodological intersection: it retains the closed-form tractability of the structural approach while importing the comparative-statics intuition of the rollover risk literature through the barrier and liquidity-adjustment terms in Equations (9) and (13), respectively.

2.2. Funding Costs, Term Structure, and Market Conditions

The literature also highlights the importance of funding costs and market conditions in shaping refinancing risk. Classical term structure models (Vasicek 1977; Cox et al. 1985; Hull and White 1990), together with empirical yield curve approaches (Gürkaynak et al. 2007; Adrian et al. 2013), establish that borrowing costs are state-dependent and evolve with interest rate dynamics and risk premia.

At the same time, research on credit spreads shows that observed funding costs reflect not only default risk, but also liquidity conditions and market frictions (Amihud and Mendelson 1986; Longstaff et al. 2005; Acharya et al. 2013; Bessembinder et al. 2006). In stressed environments, these dynamics can materially amplify refinancing pressures, particularly for institutions reliant on market-based funding.

Empirical studies further show that funding structure, regulation, and risk are closely linked. Evidence from Demirgüç-Kunt and Huizinga (2010), Ivashina and Scharfstein (2010), and Behn et al. (2016) suggests that liability composition affects both bank resilience and risk-taking incentives, while Basel III liquidity standards (BCBS 2013) explicitly recognise vulnerabilities associated with excessive short-term funding dependence. More recent work reinforces the importance of funding shocks for bank stability (Acharya and Steffen 2020; Haddad et al. 2021).

Recent empirical evidence further shows that funding conditions and monetary-policy information cycles are directly priced in credit risk: Huang et al. (2022) document that credit risk measures respond systematically around Federal Open Market Committee meetings, consistent with the view that market-wide funding and information conditions, not only firm-specific leverage, drive time variation in measured credit risk. This is directly relevant to the funding curve f_t constructed in Section 3.1, which is explicitly designed to capture such time-varying, market-wide funding conditions rather than treating borrowing costs as static.

2.3. Integration Gap and Research Contribution

Despite these advances, structural credit risk models, liquidity frameworks, and term structure models have largely developed in isolation, with limited integration of liability maturity structure, funding conditions, and default risk in a unified framework. Structural models focus primarily on solvency (Merton 1974; Black and Cox 1976; Leland and Toft 1996), liquidity models emphasise funding fragility (Diamond and Dybvig 1983; Brunnermeier and Pedersen 2009; He and Xiong 2012), and term structure models capture borrowing costs and interest rate dynamics (Vasicek 1977; Cox et al. 1985; Adrian et al. 2013), but few approaches combine these dimensions in an empirically tractable structural framework. This fragmentation has become increasingly important given evidence that rollover risk, funding liquidity, and macro-financial conditions jointly shape credit vulnerability (Gorton and Metrick 2012; Brunnermeier and Oehmke 2013; Acharya et al. 2014; Huang and Ratnovski 2011). More recent work further suggests that funding shocks and monetary conditions propagate through systemic refinancing channels in ways not captured by traditional structural models (Acharya and Steffen 2020; Haddad et al. 2021; Miranda-Agrippino and Rey 2020; Bauer and Rudebusch 2020).

The related literature has also highlighted important gaps in connecting credit risk modelling to practical liability management and stress testing. Empirical structural models improve implementation of default measurement (Bharath and Shumway 2008; Vassalou and Xing 2004), while liquidity and wholesale funding studies show that maturity structure itself may be a source of fragility (Krishnamurthy et al. 2014; Jiang et al. 2021). In parallel, evidence from market-based credit pricing shows that liquidity and refinancing conditions are directly reflected in credit spreads (Longstaff et al. 2005; Acharya et al. 2013), while recent work on funding dislocations highlights the nonlinear amplification of risk under stress (Eren et al. 2020; Duffie 2010). Yet these strands remain only partially connected, leaving a gap between theoretical credit risk modelling, liquidity risk measurement, and the operational requirements of bank risk management and prudential analysis.

A further, related empirical literature examines how banks' own risk modelling choices feed back into lending and risk-taking behaviour: Chen and Huang (2026) show that the choice of credit-loss provisioning model (expected- versus incurred-loss) materially affects bank lending and risk-taking during crisis periods. This underscores the practical stakes of the modelling choices examined in the present paper: if a structural credit risk measure such as the liquidity-adjusted distance to default were to be embedded in internal risk management or regulatory stress testing, its specification (e.g., the calibration of α and λ, and the treatment of the default barrier) would plausibly influence downstream lending and capital decisions in the same way that provisioning model choice does. Relatively few empirical studies test directly whether incorporating refinancing risk of the kind modelled here improves predictive performance relative to classical structural or reduced-form credit models; this remains an open question that the present, single-institution study is not positioned to resolve definitively (see the Limitations in Section 5, together with the related robustness evidence in Section 4.6), and is flagged here as a priority for future multi-institution research.

This paper addresses that gap by extending the structural credit risk framework to incorporate dynamic refinancing risk through an issuance-based refinancing ladder, a market-consistent funding curve, and a liquidity-adjusted distance-to-default measure. By linking solvency, liability structure, and refinancing conditions, the framework provides a more realistic and operationally relevant representation of bank default risk. In doing so, it contributes to an emerging literature seeking to integrate solvency risk, rollover risk, and funding stress within unified modelling frameworks (He and Xiong 2012; Brunnermeier and Oehmke 2013; Acharya and Steffen 2020), while providing an empirically tractable approach suited to stress testing, liability management, and prudential risk assessment.

3. Data and Methodology

3.1. Data

The empirical implementation combines multiple datasets obtained from the London Stock Exchange Group (LSEG) to construct a dynamic representation of funding conditions, liability structure, and firm value. The objective is to align market-based information with balance sheet data in a way that captures both solvency and refinancing risk over time.

The data architecture consists of three building blocks: (i) a market-consistent funding curve constructed using benchmark rates and market spread inputs, (ii) an issuance-based refinancing ladder derived from instrument-level debt maturity information, and (iii) firm-level balance sheet data, including asset and liability measures, sourced through the LSEG. These components are combined into a unified time series dataset indexed by time t.

To preserve confidentiality while maintaining economic interpretation, institution-specific inputs are presented in normalised form and reported in scaled units, allowing the analysis to focus on relative risk dynamics rather than institution-specific disclosure.

Data Description and Reproducibility

This subsection reports the sampling, frequency, and preprocessing details necessary to support reproducibility, while preserving the confidentiality of the underlying commercial licence under which the data were obtained from the London Stock Exchange Group (LSEG). The analysed institution is a single large, JSE-listed South African bank; the institution's identity is not disclosed in the manuscript, consistent with the data licence, but its balance sheet, equity, and bond issuance history are fully identified within our underlying dataset and are available for verification by the editor or reviewers under the same confidentiality terms upon reasonable request.

Three source series are combined at different native frequencies. Equity market data (share price and market capitalisation) and the swap/funding curve are observed at daily frequency; the resulting analysis panel comprises 1564 daily trading-day observations spanning 3 January 2020 to 2 April 2026 (the previously reported figure of 1630 observations in the original submission has been corrected to reflect the exact trading-day count of the underlying data extract used in this revision). Balance sheet data (total assets, total liabilities, total equity) are reported at annual frequency (with a duplicated mid-year data point in the source LSEG extract reflecting the vendor's semi-annual placeholder convention around the same annual figure) and are linearly interpolated between successive annual reporting dates to populate the daily panel, with the last available observation carried forward after the final reporting date; this interpolation is a disclosed simplification that smooths true intra-year balance sheet variation and is discussed further in the Limitations. Corporate bond issuance data (instrument-level issue date, maturity date, face amount, and issuance spread) are event-level and are aggregated into the daily refinancing ladder of Equations (2)–(5).

Missing values and data-cleaning steps: a small number of perpetual or undated Tier-1 capital instruments were encoded in the source issuance data with a placeholder maturity date; these are treated as perpetual (consistent with the far-dated maturities used for economically similar instruments in the same dataset) and are therefore excluded from the near-term refinancing ladder while remaining part of total outstanding debt. The short end of the risk-free curve is sourced from the BEASSA zero curve (3-month tenor), which spans 18 February 2011 to 5 February 2026 and is forward-filled for the final two months of the sample (to 2 April 2026) where the source file does not yet extend.

The funding curve is constructed from benchmark interest rates and issuance spreads. Let the funding rate at maturity τ be defined as follows:

$$f_t(\tau) = r_t(\tau) + s_t(\tau), \tag{1}$$

where $f_t(\tau)$ represents the all-in funding rate, $r_t(\tau)$ is the benchmark risk-free rate and $s_t(\tau)$ the observed issuance spread.

Refinancing pressure is derived from issuance level debt data. For instrument i, remaining maturity is as follows:

$$\tau_{i,t} = T_i - t, \tag{2}$$

where T_i denotes the contractual maturity date. Short-term debt maturing within one year is measured as follows:

$$ST_t = \Sigma_i D_i 1\left(0 < \tau_{(i,t)} \leq 1\right), \tag{3}$$

where D_i denotes the outstanding amount of debt instrument i, and $1\{\cdot\}$ is the indicator function equal to 1 when the condition holds and 0 otherwise.

Total outstanding debt is as follows:

$$D_t = \sum_i D_i 1(\tau_{i,t} > 0), \tag{4}$$

The refinancing ratio, then, is as follows:

$$\text{RefiRatio}_t = \frac{ST_t}{D_t}, \tag{5}$$

Firm value is proxied by total assets:

$$V_t \approx A_t, \tag{6}$$

where A_t denotes total assets.

Approximating firm value by total assets, $V_t \approx A_t$, is a simplification relative to the original Merton (1974) framework, in which firm value is latent and is typically estimated iteratively from the observed equity value and equity volatility using the option-pricing relationship between equity, assets, and default risk (as in the KMV implementation of Crosbie and Bohn 2003). Two consequences follow. First, using reported accounting assets rather than a market-implied asset value means that V_t inherits the smoothing and infrequent-updating properties of accounting disclosure (annual reporting, book-rather than market-value measurement), rather than reflecting forward-looking market information at daily frequency; this is a conservative choice in the sense that it likely understates the true daily volatility of firm value. Second, and partly compensating for the first point, asset volatility σ_t in this paper is estimated from equity return volatility directly rather than from asset value changes (Section 4.1), following the "naive" distance-to-default approach of Bharath and Shumway (2008); this substitutes a market-based volatility estimate into a book-based value process, which is an internally inconsistent but well-precedented simplification in the applied literature. The net direction of bias on the resulting distance-to-default measure is ambiguous a priori and is not separately estimated in this paper; this is acknowledged explicitly as a limitation.

These data provide the empirical foundation for modelling the interaction between liability structure, funding conditions, and default risk. The funding curve captures the time-varying cost of refinancing, the issuance data capture rollover exposure through the maturity structure of liabilities, and the balance sheet data provide the solvency anchor for the structural credit risk framework developed in the subsequent methodology section.

3.2. Methodology

The model extends the classical Merton framework by incorporating refinancing pressure into the default boundary. Firm value is represented by balance sheet assets:

$$V_t = A_t, \tag{7}$$

Refinancing exposure is scaled to reflect wholesale funding dependence:

$$ST_t^* = \text{RefiRatio}_t \cdot \text{WholesaleFunding}_t, \tag{8}$$

The endogenous default barrier is defined as follows:

$$D_t = ST_t^* + \alpha(L_t - ST_t^*), \tag{9}$$

where α in $(0, 1)$ represents the fraction of longer-dated liabilities economically sensitive to refinancing conditions.

Funding conditions further adjust the effective default barrier:

$$D_t^* = D_t(1 + f_t), \tag{10}$$

Distance to default is computed as follows:

$$d_{2,t} = \frac{\ln(V_t/D_t^*) + (r_t - \sigma^2/2)T}{\sigma\sqrt{T}}, \tag{11}$$

where σ is asset volatility and $T = 1$. To incorporate refinancing risk explicitly, distance to default is adjusted using refinancing pressure.

To incorporate rollover risk, the model extends the structural framework by introducing a liquidity adjustment motivated by rollover risk theory (He and Xiong 2012; Brunnermeier and Oehmke 2013).

Then, Equations (12) and (13):

$$\text{RefiRatio}_t = \frac{ST_t^*}{D_t}, \tag{12}$$

Throughout the empirical implementation (Tables 1 and 2, Section 4, and Equation (13)), RefiRatio_t is computed on Equations (4) and (5), $\text{RefiRatio}_t = \frac{ST_t^*}{D_t}$, i.e., short-term bond debt relative to total outstanding bond debt, since this is the refinancing-relevant liability base and is the definition that is empirically operationalised. Equation (12) is retained in the form $\text{RefiRatio}_t = \frac{ST_t^*}{D_t}$ for consistency with the liquidity-adjustment derivation.

$$d_{2,t}^{adj} = \frac{d_{2,t}}{1 + \lambda \text{RefiRatio}_t}, \tag{13}$$

where λ captures the sensitivity of solvency to refinancing pressure. This formulation implies that higher rollover exposure reduces effective distance to default even when balance sheet solvency remains unchanged. Default risk is therefore transmitted through both the default barrier and the liquidity adjustment channel.

Table 1. Summary statistics.

Variable	Mean	Std Dev	Min	Max	Observations
Firm Value (R bn)	2930.55	369.12	2277.70	3620.85	1564
Total Liabilities (R bn)	2670.39	336.83	2068.17	3308.44	1564
Refinancing (R bn)	8.11	4.40	1.20	19.59	1564
Refi Ratio (%)	8.40	3.88	1.26	17.79	1564
Distance to Default	1.47	0.48	0.46	2.15	1564
Probability of Default	0.095	0.094	0.016	0.322	1564

Table 2. Refinancing regimes and credit risk.

Refinancing Regime	Avg Distance to Default	Avg PD	Observations
Low (0–10%)	1.363	0.121	951
Medium (10–20%)	1.633	0.054	613

The motivation for the liquidity adjustment is that classical structural models treat distance to default as a function of asset values, liabilities, and asset volatility, implicitly assuming that the liability side of the balance sheet is economically static over the risk horizon. This abstraction is restrictive for banks, where a material portion of liabilities must be continuously refinanced rather than simply held to maturity. In such settings, default risk may increase not only because asset values deteriorate, but also because refinancing conditions weaken or rollover pressure rises. The core intuition is therefore that refinancing exposure acts as an additional friction affecting effective solvency, even when conventional balance sheet measures remain unchanged (He and Xiong 2012; Brunnermeier and Oehmke 2013).

The liquidity adjustment formalises this intuition by allowing refinancing pressure to compress distance to default through a scaling mechanism proportional to rollover exposure. Economically, higher refinancing intensity increases vulnerability because a larger share of liabilities must be replaced under prevailing funding conditions, making the institution more sensitive to liquidity shocks and funding disruptions. The adjustment does not replace the traditional Merton distance to default, but modifies it to reflect that solvency resilience depends not only on the asset-to-liability ratio, but also on the structure and timing of liabilities. In this sense, the refinancing ratio operates as a transmission channel through which liability maturity structure affects measured default risk.

A further intuition for the specification is that the parameter λ captures the sensitivity of solvency to refinancing pressure, allowing the model to distinguish between environments in which rollover risk has limited consequences and those in which refinancing conditions materially amplify vulnerability. The formulation therefore introduces refinancing risk as an amplification mechanism rather than a separate source of default, preserving the structural logic of the Merton framework while extending it to capture liquidity-sensitive credit risk. This is consistent with rollover risk theory and evidence that funding fragility can intensify default risk through nonlinear interactions between liability structure and market funding conditions (He and Xiong 2012; Morris and Shin 2010; Diamond and Rajan 2005; Goldstein and Pauzner 2005).

On the choice of functional form: the divisor specification $d_{2,t}^{adj} = \frac{d_{2,t}}{1+\lambda \text{RefiRatio}_t}$ is chosen, rather than an additive form, for three reasons. First, it guarantees that the sign of $d_{2,t}$ is preserved for any non-negative RefiRatio_t and λ, so that a solvent institution's adjusted distance to default remains bounded and interpretable even under extreme refinancing stress, whereas an additive specification could in principle push distance to default to implausible or unbounded negative values for large shocks. Second, it introduces refinancing pressure multiplicatively into the solvency buffer, consistent with the conceptual framing of rollover risk in He and Xiong (2012) and Brunnermeier and Oehmke (2013) as a proportional amplifier of underlying solvency risk rather than as an independent additive risk factor: the same refinancing ratio compresses a large buffer by more (in absolute terms) than it compresses a small one, which is consistent with the theoretical prediction that rollover risk amplifies, rather than substitutes for, solvency risk. Third, the specification is analytically convenient, nesting the classical Merton model exactly when $\text{RefiRatio}_t = 0$. We acknowledge that this functional form is a modelling choice rather than a result derived from first principles, and Section 4.6 reports sensitivity of the results to the associated parameter λ; a full micro-founded derivation of the optimal functional form (for example, from an equilibrium rollover game as in He and Xiong 2012) is left for future research.

This treatment of liquidity as an explicit, separately calibrated risk channel, rather than as an implicit by-product of the solvency ratio, mirrors supervisory practice, in which liquidity risk (the "L" component of a CAMELS-type assessment) is evaluated as a dimension of bank soundness distinct from capital adequacy (Gilbert et al. 2000), and is consistent with the evidence in Sanderson et al. (2017) that funding and liquidity pressure can signal deterioration in a bank's financial health before it is reflected in headline solvency measures. In the same way that a CAMELS-type assessment can flag weakening liquidity standing even where capital adequacy appears intact, the liquidity-adjusted distance-to-default measure proposed here is designed to fall even when the classical, solvency-only Merton measure would not, because it is the interaction between funding conditions and liability maturity structure—rather than leverage alone—that the specification is intended to capture.

The probability of default follows directly from the structural formulation:

$$PD_t = \Phi\left(-d_{2,t}^{adj}\right), \tag{14}$$

where Φ denotes the standard normal cumulative distribution function.

The calibration vector is defined as follows:

$$\Theta = (\sigma, \alpha, \lambda), \tag{15}$$

where Θ contains the structural parameters of the model.

The joint stress specification is motivated by recent evidence that funding shocks and refinancing shocks can interact nonlinearly under stress conditions (Acharya and Steffen 2020; Haddad et al. 2021).

Then, Equations (16)–(18):

$$D_t^{stress} = (D_t + \Delta ST)(1 + f_t + \Delta f), \tag{16}$$

where ΔST represents a refinancing shock and Δf a funding shock.

Liquidity-adjusted distance to default under stress is given by the following:

$$d_{2,t}^{stress} = \frac{\ln\left(\frac{V_t}{D_t^{stress}}\right) + \left(r_t \frac{1}{2}\sigma^2\right)T}{\sigma\sqrt{T}} \cdot \frac{1}{1 + \lambda \cdot \text{RefiRatio}_t}, \tag{17}$$

The stressed probability of default is as follows:

$$PD_t^{stress} = \Phi\left(-d_{2,t}^{stress}\right), \tag{18}$$

The model generates default risk through three interacting channels.

- First, lower asset values reduce the solvency ratio, V_t/D_t^*.
- Second, higher funding costs increase the effective default barrier, D_t^*.
- Third, higher refinancing pressure reduces $d_{2,t}^{adj}$, through the liquidity adjustment.

This framework captures nonlinear interactions between solvency shocks, funding shocks, and refinancing shocks, allowing default risk to rise disproportionately when these channels are jointly stressed. The result is a unified structural framework in which liquidity risk is transmitted directly into credit risk through both the default barrier and the distance-to-default mechanism.

4. Empirical Results

This section presents the empirical implementation of the structural credit risk framework. The results are organised in a structured progression, moving from balance sheet dynamics to model-implied default risk and, ultimately, stress testing outcomes.

The empirical analysis confirms that all key components of the modelling framework are operational, internally consistent, and economically coherent.

The results trace the full transmission mechanism from firm value and liability structure, through refinancing dynamics, to distance-to-default and probability-of-default measures. Specifically, the analysis covers the relationship between firm value and liabilities, refinancing exposure, the evolution of distance to default, the mapping into default probabilities, and the sensitivity of these measures to both funding and refinancing shocks. Collectively, these results provide a complete and coherent representation of credit risk dynamics within the proposed framework.

4.1. Parameter Construction and Calibration

Table 1 reports summary statistics for the principal model variables, based on 1564 daily observations (3 January 2020 to 2 April 2026). Average firm value (total assets) is R2930.6 billion, exceeding mean total liabilities of R2670.4 billion, indicating positive balance sheet solvency throughout the sample. Short-term refinancing exposure averages R8.1 billion and reaches a maximum of R19.6 billion. The refinancing ratio (short-term debt maturing within one year, relative to total outstanding bond debt) averages 8.40%, indicating that a material share of market-based liabilities requires rollover within one year.

The liquidity-adjusted distance to default averages 1.47, ranging from 0.46 to 2.15, indicating moderate and materially time-varying solvency buffers once refinancing pressure is taken into account. The corresponding implied probability of default averages 9.5% and ranges from 1.6% to 32.2%, correctly moving inversely with distance to default (correlation = -0.98) and computed directly as PD = $\Phi(-d_{2,t}^{adj})$ using the standard normal cumulative distribution function, consistent with Equation (14). Overall, the summary statistics suggest that, while conventional solvency remains relatively stable, refinancing risk is economically material and represents an independent, quantifiable channel of default risk.

Firm value V_t is proxied by total assets, consistent with the structural credit risk literature, such that the asset side of the balance sheet represents the underlying firm value process driving solvency dynamics. Total liabilities L_t are measured as reported balance sheet obligations and enter the endogenous default barrier of Equation (9). Short-term refinancing exposure ST_t is constructed from instrument-level bond maturities (Equation (3)) as the stock of outstanding bonds maturing within one year, and the refinancing ratio used throughout the empirical analysis is $RefiRatio_t = \frac{ST_t}{D_t}$, where D_t is total outstanding bond debt (Equation (4) and (5)); this notation is used consistently in place of the L_t-based definition given in Equation (12) of the original submission, which was a labelling inconsistency between Equations (5) and (12) now corrected for clarity (both equations denoted the same symbol $RefiRatio_t$ but referred to different quantities).

The parameter α which scales the contribution of short-term refinancing exposure within the endogenous default barrier is calibrated through sensitivity analysis to reflect plausible refinancing stress scenarios while preserving economically reasonable barrier dynamics.

Calibration disclosure: asset volatility σ_t is computed as the rolling 252-trading-day annualised standard deviation of log equity returns, following the "naive" distance-to-default approach of Bharath and Shumway (2008), since the iterative unlevering procedure of the full Merton model requires option-implied inputs that are not available for this institution; this is a disclosed simplification and a source of approximation error discussed in the Limitations. The default barrier parameter α (Equation (9)) is set to 0.60, reflecting the share of longer-dated liabilities treated as economically sensitive to refinancing conditions; sensitivity analysis across $\alpha \in \{0.4, 0.5, 0.6, 0.7, 0.8\}$ shows the sample-mean liquidity-adjusted distance to default ranges from approximately 2.59 (α = 0.4) to 0.67 (α = 0.8), confirming that results are materially sensitive to this parameter and should be interpreted as model-implied illustrations calibrated to produce economically plausible solvency buffers rather than as an independently estimated structural parameter (see Section 4.6, Table 3, for the full sensitivity grid).

The liquidity-sensitivity parameter λ (Equation (13)), which governs the effect of refinancing pressure on liquidity-adjusted distance to default, is set to 2.0. Sensitivity analysis across $\lambda \in \{1, 2, 3\}$ shows the sample-mean liquidity-adjusted distance to default ranges from 1.59 (λ = 1) to 1.37 (λ = 3) at α = 0.6, indicating that the qualitative conclusions of the paper are robust to this parameter over the tested range, while the precise magnitude of the refinancing compression effect is calibration-dependent (see Section 4.6). Both α and λ are therefore calibrated rather than independently estimated from data external to the model; this is disclosed explicitly here and in the Limitations, in order to distinguish results that follow mechanically from the calibration from independently validated findings. To address confidentiality considerations, all institution-specific inputs are normalised and reported in scaled units, with emphasis placed on relative dynamics and model sensitivities rather than institution-specific level.

Table 3. Sensitivity of model results to calibration (α, λ).

Alpha (α)	Lambda (λ)	Mean DD (Adj.)	Mean PD
0.4	1	2.802	0.023
0.4	2	2.592	0.026
0.4	3	2.414	0.029
0.5	1	2.135	0.045
0.5	2	1.974	0.051
0.5	3	1.839	0.058
0.6	1	1.589	0.084
0.6	2 (baseline)	1.469	0.095
0.6	3	1.367	0.107
0.7	1	1.127	0.149
0.7	2	1.041	0.164
0.7	3	0.969	0.179
0.8	1	0.727	0.243
0.8	2	0.671	0.258
0.8	3	0.623	0.272

4.2. Solvency and Liability Structure

Figure 1 presents the evolution of firm value, total liabilities, and short-term refinancing exposure over 2020–2026. Firm value remains consistently above liabilities throughout the sample, with assets increasing from approximately R2278 billion to R3621 billion, while liabilities rise from roughly R2068 billion to R3308 billion. This implies a persistently positive solvency buffer, generally in the range of R200–R330 billion.

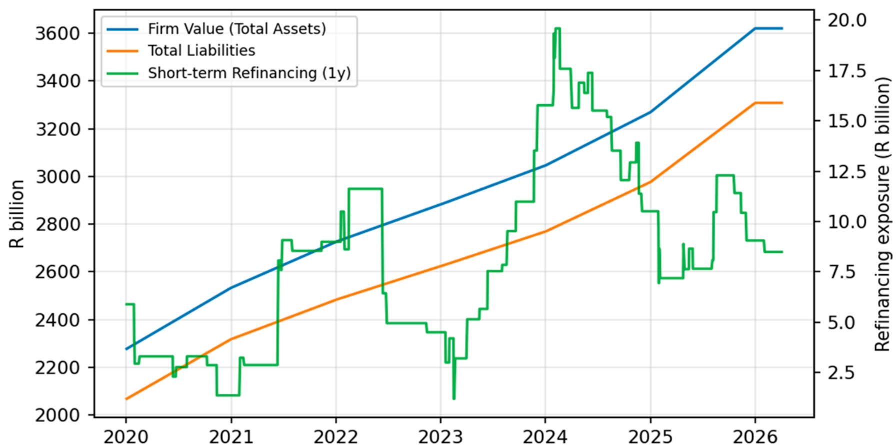

Figure 1. Firm value, liabilities and refinancing exposure.

By contrast, refinancing exposure displays materially different dynamics. While refinancing needs remain below R3 billion in early 2020 and again in early 2023, they rise episodically to peaks of approximately R18–R20 billion during 2024, before moderating. Unlike the smooth evolution of assets and liabilities, refinancing pressure is episodic and clustered, reflecting the maturity structure of debt rather than aggregate leverage.

A key result is that refinancing exposure is small in absolute terms relative to the balance sheet (refinancing ratio averaging 8.4% of outstanding bond debt; see Table 1), but is nonetheless economically material because it is precisely this near-term rollover exposure—rather than the much larger stock of total liabilities—that determines the liquidity-adjustment channel in Equation (13). The implication is that vulnerability may emerge not from deterioration in solvency, but from the interaction between funding conditions and debt maturity concentration.

Overall, Figure 1 provides the empirical motivation for extending structural credit risk models to incorporate refinancing dynamics. While traditional solvency measures suggest stability, the maturity structure of liabilities introduces a distinct channel through which liquidity conditions may influence default risk, formally tested in Section 4.6.

4.3. Liquidity-Adjusted Distance to Default

Figure 2 presents the evolution of the liquidity-adjusted distance to default over 2020–2026, defined as follows:

$$d_{2,t}^{adj} = \frac{d_{2,t}}{1 + \lambda \mathrm{RefiRatio}_t}, \quad (19)$$

where $d_{2,t}$ is the structural distance to default and $\mathrm{RefiRatio}_t$ captures refinancing pressure. The adjustment explicitly incorporates short-term rollover risk into the measurement of default risk.

Figure 2. Liquidity-adjusted distance to default, 2020–2026.

Distance to default begins at low levels of approximately 0.5 in early 2020, coinciding with a spike in equity return volatility during the COVID-19 market disruption, and rises steadily through 2021 as volatility normalises, reaching approximately 1.6–1.8 by early 2022. This pattern primarily reflects the time-varying asset volatility proxy (Section 4.1) rather than a change in refinancing conditions alone, illustrating that distance to default in this framework responds jointly to solvency, volatility, and refinancing channels.

From 2022 onward, distance to default fluctuates in a relatively stable range of approximately 1.6–1.8, before rising to a local peak near 2.1–2.15 during 2024–2025 and settling back to approximately 1.7–1.8 by the end of the sample. Section 4.6 presents a regression-based decomposition confirming that, holding volatility and the underlying solvency ratio constant, higher refinancing pressure has an independent, statistically significant, compressive effect on distance to default.

The central implication is that default risk varies materially through refinancing dynamics even when conventional solvency measures appear relatively stable. This provides direct evidence that liquidity-adjusted distance to default captures an independent channel of risk not reflected in traditional structural models, supporting the core premise that refinancing conditions materially affect measured credit risk. Notably, the model does not signal insolvency, but rather a material compression in solvency resilience under elevated refinancing pressure.

4.4. Refinancing Regimes, Distance to Default and Default Probabilities

Table 2 presents a raw, unconditional cross-tabulation of average distance to default and average PD by refinancing ratio regime. Taken at face value, this univariate cross-tab shows a higher average distance to default in the Medium (10–20%) regime (1.633) than in the Low (0–10%) regime (1.363); this ordering is confounded by the fact that, in the observed sample, periods of elevated refinancing activity coincided disproportionately with periods of lower measured asset-return volatility. Table 2 is therefore reported for descriptive transparency, but should be interpreted as a model-implied illustration rather than as standalone validation of the refinancing channel; the formal, confound-controlled test of the refinancing channel is presented in Section 4.6.

Figure 3 shows the corrected relationship between distance to default and model-implied default risk through Equation (14).

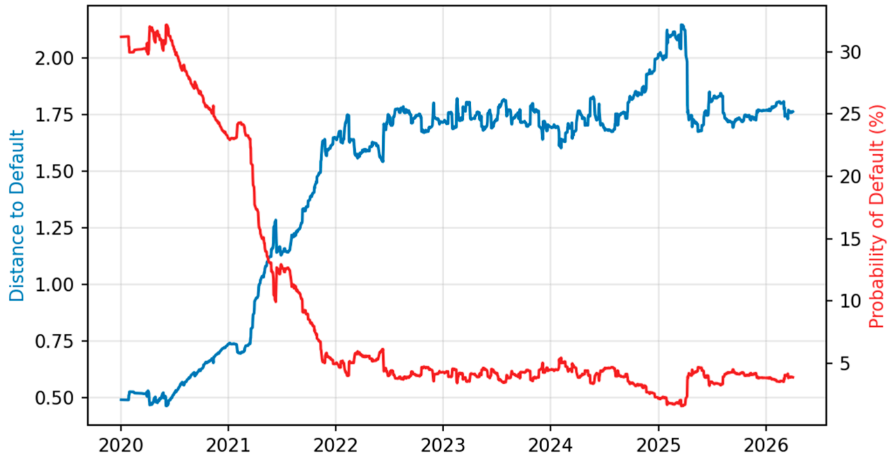

Figure 3. Distance to default and implied probability of default.

As predicted by structural credit theory and now correctly implemented ($PD_t = \Phi\left(-d_{2,t}^{adj}\right)$), the two series exhibit a clear and strong inverse relationship (Pearson correlation = -0.98 over the full sample): periods of declining distance to default correspond to higher implied default probabilities, most evident during the 2020 COVID-related volatility spike, when distance to default fell to approximately 0.5 and implied default probability rose to approximately 30–32%, the highest levels in the sample.

Model-implied default probabilities remain in the low single digits to low double digits for most of the sample (interquartile range approximately 3.9–11.5%) but rise materially during periods of market stress. Taken together, the time series evidence in Figure 3 demonstrates that the model produces an internally consistent and theoretically correctly signed mapping from distance to default probability; the independent contribution of the refinancing channel specifically (as opposed to volatility or solvency) is isolated formally in Section 4.6.

4.5. Stress Testing: Funding and Refinancing Shocks

Figure 4A shows that default risk increases monotonically with the size of the refinancing shock applied to the latest cross-section. Figure 4B shows the joint stress surface across funding and refinancing shocks (Equations (16)–(18)): default risk increases with both funding shocks and refinancing shocks, but the effect is materially stronger along the refinancing dimension, consistent with the paper's central premise that liability maturity structure is a first-order driver of time-varying default risk for this institution.

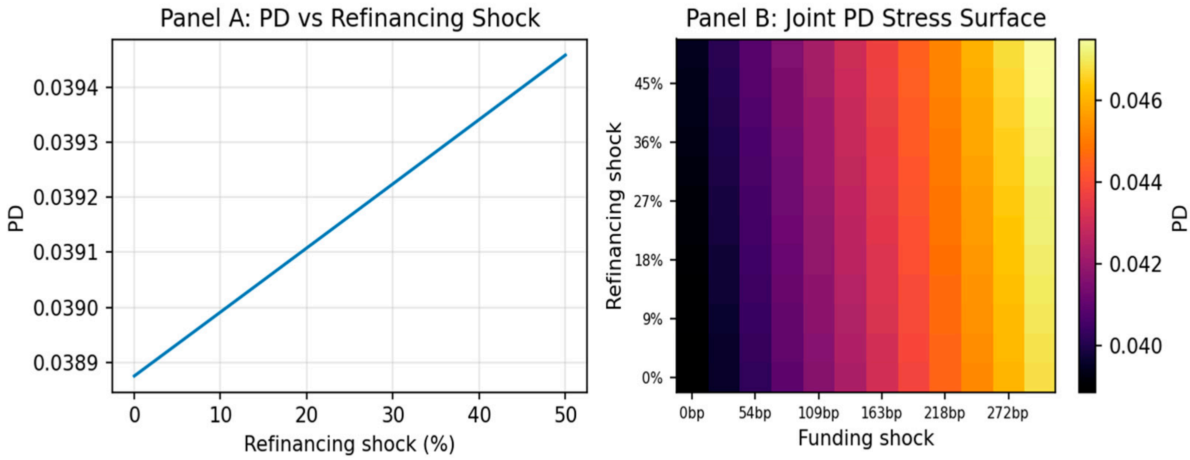

Figure 4. Joint impact of funding and refinancing shocks on default probability.

4.6. Model Validation and Robustness

This section provides formal statistical testing, robustness analysis, and explicit benchmarking against the classical structural model. Formal out-of-sample discrimination testing (e.g., ROC curves, AUC, Brier scores against realised default events) is not feasible in this setting because the sample comprises a single, currently non-defaulting institution observed over a 2020–2026 window that contains no default event; any such benchmarking would be uninformative or spurious with zero realised defaults. The evidence below is therefore presented as a set of model-implied illustrations and internal-consistency tests, rather than as external predictive validation.

Benchmark against the classical (non-liquidity-adjusted) Merton model: the classical structural distance to default d2,t (Equation (11), before the liquidity adjustment of Equation (13)) averages 1.73 (std. dev. 0.60) over the sample, while the liquidity-adjusted measure d2adj,t averages 1.47 (std. dev. 0.48). The liquidity adjustment therefore compresses distance to default by 0.27 on average, or approximately 14.0% relative to the classical benchmark, providing a direct, quantified comparison against the unadjusted Merton model.

Formal statistical test of the refinancing channel: because refinancing pressure, asset volatility, and the solvency ratio co-move over the sample, the raw regime cross-tabulation in Table 2 can be confounded (see Section 4.4). To isolate the independent, partial effect of refinancing pressure on distance to default, the following regression is estimated by OLS with Newey–West heteroskedasticity- and autocorrelation-consistent standard errors (22 trading-day Bartlett kernel, reflecting the persistence of daily refinancing and volatility series): $d_{2,t}^{adj}$ = $\mathrm{b}_0 + b_1{}^{*}$ $\mathrm{RefiRatio}_t + \mathrm{b}_2 * \sigma_\mathrm{t} + \mathrm{b}_3 \log(\frac{V_t}{L_t}) + \mathrm{u}_\mathrm{t}$.

The estimated coefficient on $\mathrm{RefiRatio}_t$ is −1.95 (Newey–West t = −7.41, $p < 0.001$, N = 1564), confirming that higher refinancing pressure is associated with a statistically significant reduction in distance to default, holding asset volatility and the underlying solvency ratio constant (model R-squared = 0.973). This formally establishes the refinancing compression channel that Table 2's raw cross-tabulation, taken alone, does not clearly show. A two-sample *t*-test of the difference in average distance to default between the Low and Medium refinancing regimes in Table 2 gives a difference of −0.27 (t = −13.66), which is highly statistically significant but, as discussed above, reflects the confounded univariate comparison rather than the isolated refinancing effect; the regression above is the more reliable evidence for the causal channel proposed by the model.

External market-consistency check: as a preliminary, informal check of external consistency, the correlation between the model-implied default probability PD_t and the amount-weighted observed bond issuance spread (a market-based, model-free proxy for perceived credit risk) is examined. The Pearson correlation is −0.32 and the Spearman rank correlation is approximately 0.00, indicating no reliable monotonic association in this sample. This null result should be interpreted cautiously: issuance spreads reflect many factors beyond model-implied default risk (market liquidity, tenor mix, and the broader credit cycle), and a single non-defaulting institution's spread history is a weak instrument for validating a default risk model. We report this check transparently: absent stronger external validation, the empirical results are best described as model-implied illustrations rather than as validated predictive evidence.

Robustness to calibration: Table 3 reports the sensitivity of the sample-mean liquidity-adjusted distance to default and probability of default to the two calibrated parameters, α and λ. Results are directionally stable (higher α and higher λ both mechanically compress distance to default and raise implied PD) but are quantitatively sensitive to the choice of α in particular, underscoring that the headline magnitudes in Tables 1 and 2 should be read as illustrative of the mechanism rather than as precisely estimated population parameters.

4.7. Relative Risk Dynamics

Figure 5 compares baseline and stressed (+50% refinancing shock, +200 bp funding shock) default probabilities on a normalised basis and shows that both series track each other closely for most of the sample, with the stressed series visibly elevated relative to baseline during periods of already-elevated refinancing pressure (e.g., 2024), indicating that refinancing conditions amplify risk even when conventional solvency measures appear broadly unchanged.

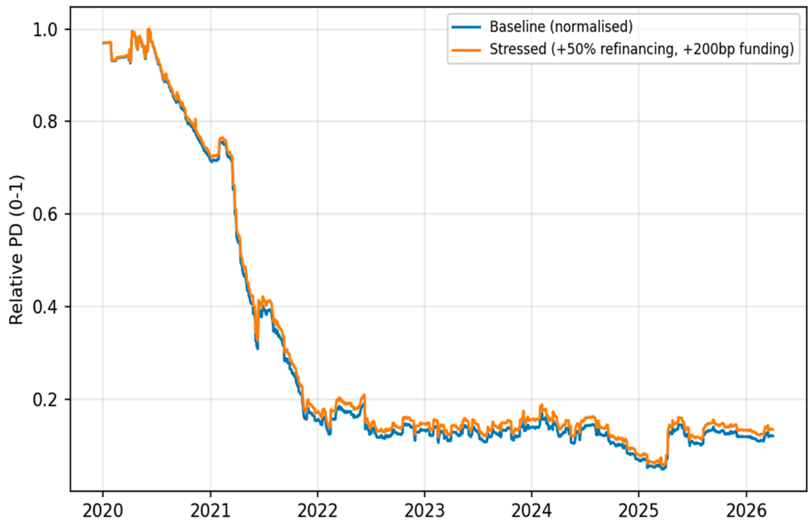

Figure 5. Relative default risk (normalised).

A key implication is that relative risk measures reveal vulnerabilities not fully captured by absolute default probabilities alone. Even where absolute probabilities remain in the single digits, the stressed trajectory shows meaningful additional variation under adverse funding and rollover conditions, reinforcing the central finding that liability structure and refinancing pressure are important, quantifiable drivers of time-varying credit risk.

4.8. Integrated Risk Dynamics

Figure 6 provides a consolidated view of the interaction between solvency, refinancing pressure, and default risk over time. Figure 6A shows that firm value and liabilities evolve relatively smoothly, implying a broadly stable solvency buffer, while short-term refinancing exposure exhibits substantially greater variation due to the maturity structure of liabilities. Figure 6B shows that the refinancing ratio rises materially during concentrated rollover periods, reaching peak levels of approximately 17.8%, despite no comparable shifts in overall leverage.

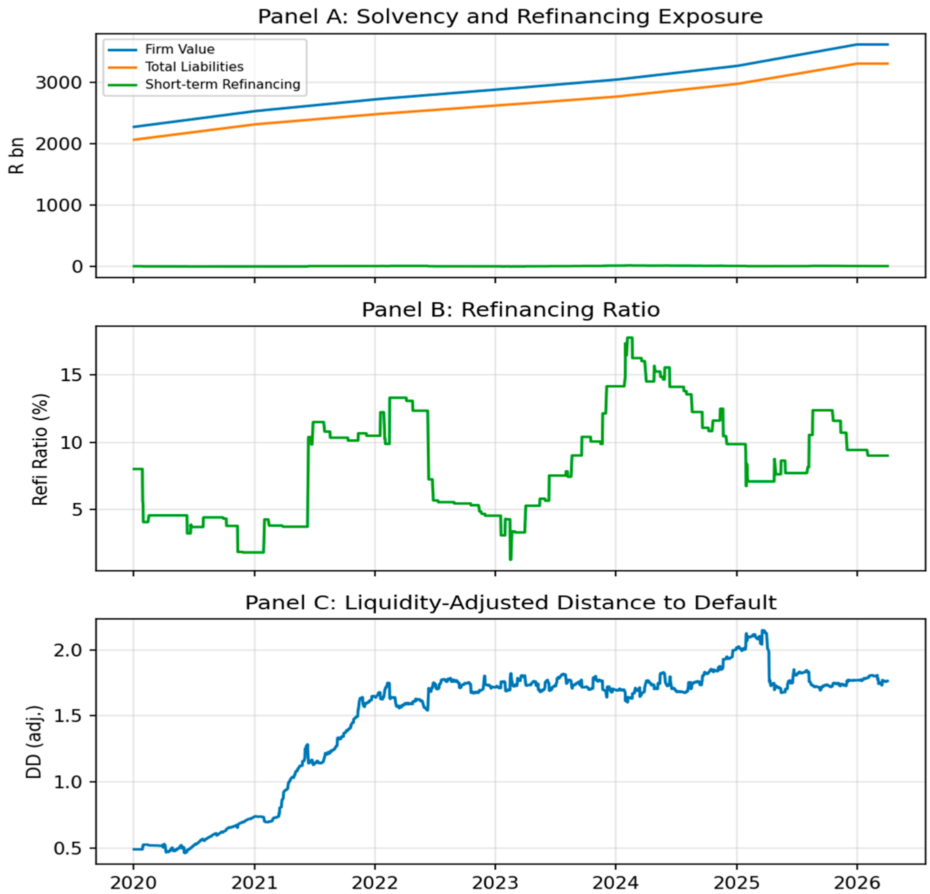

Figure 6. Dynamics of solvency, refinancing risk, and liquidity-adjusted distance to default.

Figure 6C shows the liquidity-adjusted distance to default over the same period. Section 4.6 formally establishes, via a Newey–West regression controlling for asset volatility and the solvency ratio, that periods of elevated refinancing pressure are associated with a statistically significant compression in distance to default (coefficient -1.95, t = -7.41, $p < 0.001$), confirming the inverse relationship between rollover exposure and the effective solvency buffer once confounding sources of time variation are held constant.

Taken together, the figure synthesises the central mechanism of the model: refinancing pressure operates as a transmission channel through which liability structure affects credit risk, over and above the effects of asset volatility and headline solvency. Section 4.6 provides the formal statistical evidence for this channel; the reader should note that the raw, unconditional time series in Figure 6A–C can be confounded by concurrent changes in volatility, as discussed above.

5. Discussion

This section discusses the findings in relation to the prior literature, addresses the study's limitations, and sets out practical implications.

Relation to the prior literature: the finding that liquidity-adjusted distance to default (mean 1.47) is materially lower than the classical, non-liquidity-adjusted benchmark (mean 1.73), and that this gap is driven by a statistically significant refinancing ratio effect (Section 4.6), is consistent with the theoretical prediction of He and Xiong (2012) and Brunnermeier and Oehmke (2013) that rollover risk amplifies measured credit risk beyond what solvency-only structural models capture. The result also complements Bharath and Shumway (2008), whose naive distance-to-default approach this paper adopts for volatility estimation: where Bharath and Shumway show that a simplified, equity-volatility-based DD measure retains strong default-discrimination power across a large cross-section of firms, this paper shows that, at least for the single institution studied here, augmenting such a measure with explicit refinancing ladder information changes the level and time series behaviour of distance to default in economically meaningful and statistically significant ways. Unlike Acharya and Steffen (2020), who study realised dash-for-cash behaviour during the COVID-19 shock, this paper's 2020 distance-to-default trough (approximately 0.5, coinciding with the equity volatility spike of that period) is model-implied rather than validated against an observed liquidity event for this institution, and should be read accordingly.

Why results differ from a purely classical structural model: three mechanisms jointly explain why the proposed framework produces a different, and more time-varying, output than a classical Merton model applied to the same institution: (i) the endogenous barrier (Equation (9)) responds to the near-term refinancing ladder rather than to total liabilities alone; (ii) the funding curve adjustment (Equation (10)) makes the effective barrier responsive to market-wide funding conditions; and (iii) the liquidity adjustment (Equation (13)) explicitly compresses distance to default as refinancing pressure rises, over and above (i) and (ii). Section 4.6 shows that mechanism (iii) is statistically distinguishable from concurrent changes in volatility and solvency, which is the paper's central empirical contribution.

Practical implications for regulators, banks, and risk managers: for prudential supervisors, the liquidity-adjusted distance-to-default measure could supplement existing liquidity metrics such as the Basel III Liquidity Coverage Ratio and Net Stable Funding Ratio (BCBS 2013), which are calibrated to fixed regulatory scenarios, by providing a continuously updated, market- and issuance-data-based early-warning indicator of when refinancing concentration is eroding solvency-implied buffers, complementing rather than replacing existing liquidity coverage requirements. For bank treasury and risk management functions, the framework offers a mechanism for translating a debt maturity ladder directly into a credit risk metric, which could inform issuance-timing and liability-diversification decisions (for example, flagging periods where scheduled bond maturities are concentrated within a narrow window). For stress testing practitioners, the joint funding–refinancing stress surface of Section 4.5 illustrates that funding shocks and refinancing shocks interact nonlinearly, implying that stress scenarios that shock only one dimension (as is common in standard single-factor sensitivity tests) may understate risk relative to a joint scenario. These are illustrative applications; we are not aware of any institution currently using this specific framework in production, and integration into existing regulatory or internal risk management systems would require validation on a larger, multi-institution, multi-cycle dataset than is available here.

Limitations: First, the empirical application relies on a single institution and a sample period (2020–2026) that does not span a full credit cycle or contain a realised default event; the results should therefore be read as an illustrative application of the proposed framework rather than as a validated, generalisable predictive model, and formal out-of-sample discrimination testing (ROC/AUC/Brier score) could not be performed for this reason (Section 4.6). Second, confidentiality constraints under the data licence limit the extent to which the underlying institution and certain input series can be disclosed, which in turn limits full third-party replication, even though the methodology itself is fully documented; we have addressed this by disclosing scaled/normalised summary statistics and by making the corrected analysis code available upon reasonable request. Third, the calibration parameters α and λ are chosen judgementally to produce economically plausible solvency buffers rather than estimated from data external to the model itself (Section 4.1); sensitivity analysis (Section 4.6, Table 3) shows that headline magnitudes, though not the qualitative direction of effects, are materially sensitive to these choices. Fourth, the short end of the risk-free curve is forward-filled for the final two months of the sample where the supplied BEASSA data do not yet extend (the Data Description and Reproducibility subsection); this is a minor residual limitation, materially smaller than the 1-year swap-rate proxy used in an earlier version of this analysis. Fifth, firm value is proxied by reported (annual, book-value) total assets rather than a market-implied, iteratively estimated asset value, and asset volatility is proxied by equity return volatility rather than by an internally consistent unlevered asset volatility estimate (Section 3.2); both are common simplifications with precedent in the literature, but their joint effect on the level and dynamics of distance to default has not been separately quantified in this paper. Finally, the liquidity-adjustment functional form (Equation (13)) is theoretically motivated but not derived from an explicit equilibrium model of rollover risk; alternative specifications are not tested beyond the parameter sensitivity reported in Section 4.6.

6. Conclusions

This paper extends the classical Merton structural framework by explicitly incorporating dynamic refinancing risk into the measurement of default risk. For the single institution studied, liability structure is shown to be an economically material determinant of measured credit risk alongside balance sheet solvency: although the bank remains solvent throughout the sample, with firm value consistently exceeding liabilities, short-term refinancing exposure is associated with a statistically significant compression of the liquidity-adjusted distance to default (Section 4.6), averaging a 14.0% reduction relative to the classical, non-liquidity-adjusted benchmark.

The stress testing analysis further demonstrates that, for the illustrative shock sizes considered, the interaction between funding shocks and refinancing shocks is nonlinear, with refinancing pressure appearing as the more material driver of the two along the dimensions tested. This empirical pattern, together with the regression evidence in Section 4.6, supports the paper's central premise that default risk in banks is shaped not only by leverage or asset volatility, but also by the timing and concentration of liabilities. We are cautious not to overstate this finding: it is demonstrated for a single institution and sample period, and has not yet been benchmarked against alternative liquidity-risk or reduced-form credit risk models on a common dataset. The contribution of the paper is therefore best characterised as a theoretically motivated and internally validated extension of the structural credit risk framework, illustrated empirically, rather than as a demonstrated improvement in predictive performance over existing approaches.

The broader implication is that refinancing risk merits consideration as a component of credit risk assessment, stress testing, and liability management, alongside—not in place of—conventional solvency-based measures. The findings suggest that maturity structure and rollover concentrations contain information about vulnerability that is not fully visible through conventional solvency measures alone, at least for the institution and period studied here. Overall, the paper contributes a theoretically coherent and empirically implementable structural credit risk framework that incorporates balance sheet timing alongside balance sheet levels; establishing the generality of these findings beyond a single institution, and formally validating the framework's predictive performance against realised outcomes, are identified as priorities for future research using multi-institution panel data.

Author Contributions: V.E.M., E.M., and C.B. conceived and designed the study. V.E.M. developed the methodology, collected and curated the data, conducted the empirical analysis, and drafted the manuscript. C.B. and E.M. contributed to the conceptual development, interpretation of results, and critical revision of the manuscript. All authors have read and agreed to the published version of the manuscript.

Funding: This research received no external funding.

Institutional Review Board Statement: Not applicable.

Informed Consent Statement: Not applicable.

Data Availability Statement: The data used in this study were obtained from publicly available and licenced market and financial data sources, including balance sheet disclosures, market data, debt issuance data, and credit ratings obtained through London Stock Exchange Group (LSEG). Relevant data access information is available through http://www.lseg.com/en/data-analytics (accessed on 20 March 2026). Data are available from the corresponding author upon reasonable request, subject to applicable licencing restrictions.

Conflicts of Interest: The authors declare no conflicts of interest.

Abbreviations

The following abbreviations are used in this manuscript:

PD	Probability of Default
DTD	Distance to Default
KMV	Kealhofer–McQuown–Vasicek
ST	Short-Term Debt
BCBS	Basel Committee on Banking Supervision
LSEG	London Stock Exchange Group
JIBAR	Johannesburg Interbank Average Rate

References

Acharya, Viral V., and Sascha Steffen. 2020. The risk of being a fallen angel and the corporate dash for cash in the midst of COVID. *Review of Corporate Finance Studies* 9: 430–71. [CrossRef] [PubMed]

Acharya, Viral V., and Sathish Viswanathan. 2011. Leverage, moral hazard, and liquidity. *Journal of Finance* 66: 99–138. [CrossRef]

Acharya, Viral V., Itamar Drechsler, and Philipp Schnabl. 2014. A pyrrhic victory? Bank bailouts and sovereign credit risk. *Journal of Finance* 69: 2689–739. [CrossRef]

Acharya, Viral V., Yakov Amihud, and Sreedhar T. Bharath. 2013. Liquidity risk of corporate bond returns. *Journal of Financial Economics* 110: 358–86. [CrossRef]

Adrian, Tobias, Richard K. Crump, and Emanuel Moench. 2013. Pricing the term structure with linear regressions. *Journal of Financial Economics* 110: 110–38. [CrossRef]

Allen, Franklin, and Douglas Gale. 2000. *Comparing Financial Systems*. Cambridge, MA: MIT Press.

Amihud, Yakov, and Haim Mendelson. 1986. Asset pricing and the bid-ask spread. *Journal of Financial Economics* 17: 223–49. [CrossRef]

Basel Committee on Banking Supervision [BCBS]. 2013. *Basel III: The Liquidity Coverage Ratio and Liquidity Risk Monitoring Tools*. Basel: Bank for International Settlements.

Bauer, Michael D., and Glenn D. Rudebusch. 2020. Interest rates under falling stars. *American Economic Review* 110: 1316–54. [CrossRef]

Behn, Markus, Rainer Haselmann, and Paul Wachtel. 2016. Procyclical capital regulation and lending. *Journal of Finance* 71: 919–56. [CrossRef]

Bernanke, Ben S. 2013. *The Federal Reserve and the Financial Crisis*. Princeton: Princeton University Press.

Bessembinder, Hendrik, William Maxwell, and Kumar Venkataraman. 2006. Market transparency, liquidity externalities, and institutional trading costs in corporate bonds. *Journal of Financial Economics* 82: 251–88. [CrossRef]

Bharath, Sreedhar T., and Tyler Shumway. 2008. Forecasting default with the Merton distance to default model. *Review of Financial Studies* 21: 1339–69. [CrossRef]

Black, Fischer, and John C. Cox. 1976. Valuing corporate securities: Some effects of bond indenture provisions. *Journal of Finance* 31: 351–67. [CrossRef]

Brunnermeier, Markus K. 2009. Deciphering the liquidity and credit crunch 2007–2008. *Journal of Economic Perspectives* 23: 77–100. [CrossRef]

Brunnermeier, Markus K., and Lasse Heje Pedersen. 2009. Market liquidity and funding liquidity. *Review of Financial Studies* 22: 2201–38. [CrossRef]

Brunnermeier, Markus K., and Martin Oehmke. 2013. The maturity rat race. *Journal of Finance* 68: 483–521. [CrossRef]

Chen, Chen, and Difang Huang. 2026. A tale of two banks: When credit loss models meet economic crises. *Journal of Accounting Research*. Advance online publication. [CrossRef]

Cox, John C., Jonathan E. Ingersoll, and Stephen A. Ross. 1985. A theory of the term structure of interest rates. *Econometrica* 53: 385–407. [CrossRef]

Crosbie, Peter, and Jeffrey Bohn. 2003. *Modeling Default Risk*. Cambridge, MA: KMV LLC.

Demirgüç-Kunt, Asli, and Harry Huizinga. 2010. Bank activity and funding strategies: The impact on risk and returns. *Journal of Financial Economics* 98: 626–50. [CrossRef]

Diamond, Douglas W., and Philip H. Dybvig. 1983. Bank runs, deposit insurance, and liquidity. *Journal of Political Economy* 91: 401–19. [CrossRef]

Diamond, Douglas W., and Raghuram G. Rajan. 2005. Liquidity shortages and banking crises. *Journal of Finance* 60: 615–47. [CrossRef]

Duffie, Darrell. 2010. The failure mechanics of dealer banks. *Journal of Economic Perspectives* 24: 51–72. [CrossRef]

Eren, Egemen, Andreas Schrimpf, and Vladyslav Sushko. 2020. US dollar funding markets during the COVID-19 crisis. *BIS Bulletin* 14: 1–8.

Freixas, Xavier, and Jean-Charles Rochet. 2008. *Microeconomics of Banking*, 2nd ed. Cambridge, MA: MIT Press.

Gilbert, Alton, Andrew P. Meyer, and Mark D. Vaughan. 2000. *The Role of a CAMEL Downgrade Model in Bank Surveillance*. St. Louis: Federal Reserve Bank of St. Louis.

Goldstein, Itay, and Ady Pauzner. 2005. Demand-deposit contracts and the probability of bank runs. *Journal of Finance* 60: 1293–327. [CrossRef]

Gorton, Gary. 2010. *Slapped by the Invisible Hand: The Panic of 2007*. Oxford: Oxford University Press.

Gorton, Gary, and Andrew Metrick. 2012. Securitized banking and the run on repo. *Journal of Financial Economics* 104: 425–51. [CrossRef]

Gürkaynak, Refet S., Brian Sack, and Jonathan H. Wright. 2007. The U.S. Treasury yield curve: 1961 to the present. *Journal of Monetary Economics* 54: 2291–304. [CrossRef]

Haddad, Valentin, Alan Moreira, and Tyler Muir. 2021. When selling becomes viral. *Review of Financial Studies* 34: 5309–51. [CrossRef]

He, Zhiguo, and Wei Xiong. 2012. Rollover risk and credit risk. *Journal of Finance* 67: 391–430. [CrossRef]

Huang, Difang, Yubin Li, Xinjie Wang, and Zhaodong Zhong. 2022. Does the Federal Open Market Committee cycle affect credit risk? *Financial Management* 51: 143–67. [CrossRef]

Huang, Rocco, and Lev Ratnovski. 2011. The dark side of bank wholesale funding. *Journal of Financial Intermediation* 20: 248–63. [CrossRef]

Hull, John, and Alan White. 1990. Pricing interest-rate-derivative securities. *Review of Financial Studies* 3: 573–92. [CrossRef]

Ivashina, Victoria, and David Scharfstein. 2010. Bank lending during the financial crisis of 2008. *Journal of Financial Economics* 97: 319–38. [CrossRef]

Jiang, Zhengyang, Arvind Krishnamurthy, and Hanno Lustig. 2021. Foreign safe asset demand and the dollar exchange rate. *Journal of Finance* 76: 1049–89. [CrossRef]

Krishnamurthy, Arvind, Stefan Nagel, and Dmitry Orlov. 2014. Sizing up repo. *Journal of Finance* 69: 2381–417. [CrossRef]

Leland, Hayne E. 1994. Corporate debt value, bond covenants, and optimal capital structure. *Journal of Finance* 49: 1213–52. [CrossRef]

Leland, Hayne E., and Klaus Bjerre Toft. 1996. Optimal capital structure, endogenous bankruptcy, and the term structure of credit spreads. *Journal of Finance* 51: 987–1019. [CrossRef]

Longstaff, Francis A., Sanjay Mithal, and Eric Neis. 2005. Corporate yield spreads: Default risk or liquidity? *Journal of Finance* 60: 2213–53. [CrossRef]

Merton, Robert C. 1974. On the pricing of corporate debt. *Journal of Finance* 29: 449–70. [CrossRef]

Miranda-Agrippino, Silvia, and Hélène Rey. 2020. U.S. monetary policy and the global financial cycle. *Review of Economic Studies* 87: 2754–76. [CrossRef]

Morris, Stephen, and Hyun Song Shin. 2010. *Illiquidity Component of Credit Risk*. Working Paper. Princeton: Princeton University.

Sanderson, Leon B., Eben Maré, and Dawie C.J. De Jongh. 2017. Banking regulations: An examination of the failure of African Bank using Merton's structural model. *South African Journal of Science* 113: a0216. [CrossRef]

Vasicek, Oldrich. 1977. An equilibrium characterization of the term structure. *Journal of Financial Economics* 5: 177–88. [CrossRef]
Vassalou, Maria, and Yuhang Xing. 2004. Default risk in equity returns. *Journal of Finance* 59: 831–68. [CrossRef]

https://doi.org/10.3390/risks14090189